JOURNAL OF THEORETICAL
AND APPLIED MECHANICS
40, 4, pp. 1021-1049, Warsaw 2002

STABILITY OF ROTATING SHAFTS MADE OF PIEZOELECTRIC FIBER COMPOSITES

PIOTR M. PRZYBYŁOWICZ

Institute of Machine Design Fundamentals, Warsaw University of Technology
e-mail: piotrp@ipbm.simr.pw.edu.pl

In the paper, theoretical fundamentals of stabilisation of a rotating shaft by making use of piezoelectric elements are presented. The shaft is made of an active piezoelectric fiber composite – the state-of-the-art structural material which has just emerged in the field of "smart" engineering. Irrespective of the kind of material the rotating shafts are made of, they exhibit flutter-type instability brought about by the presence of internal friction. At a certain critical rotation speed the system loses its stability and starts to perform self-excited vibrations. The paper discusses a method protecting the shaft from such a phenomenon or, at least, shifting it away by incorporation of piezoelectric fibers embedded in a polymer matrix and electrodes bonded to each lamina of the active composite. The constitutive equations of the laminate are derived and used in formulation of equations of motion of the rotating shaft. The analysis of stabilisation reveals that the desired effect can be achieved by application of three and more pairs of the electrodes enabling generation of a constant bending moment regardless of the rotary motion. Proportional and velocity feedbacks in the control system are examined and compared. The critical threshold is determined by investigating the eigenvalues corresponding to the governing equations linearised around non-trivial equilibrium position. The equations themselves were earlier found via a uni-modal Galerkin's discretisation of the partial differential equations of motion. The applied method proves to be efficient as, an increase in the critical speed by two and more times is observed after activation of the proposed stabilisation method.

Key words: rotating shaft, stabilisation, active composites, piezoelectric elements

1. Introduction

Problems of rotor dynamics have been thoroughly examined by numerous authors but one of the most complete descriptions can be found in works

by Muszyńska (1971, 1976) and Tondl (1965), who paid attention to the modelling and analysis of flexible shafts undergoing force, parametric, and self-excitations. Those works give also a plenteous literature survey and feature generality of non-linear models of rotor supports as well as models of internal friction.

Rotating shafts, even when perfectly balanced, exhibit self-excited vibration brought about by internal dissipation due to internal friction, structural friction in articulated joints, etc. The instability occurs while exceeding the critical rotation speed (over the first eigenfrequency corresponding to flexural vibration of the given shaft as a beam), and is manifested by sudden growth in the amplitude of transverse vibration for a slight change of the rotation speed. It is to be emphasised that the mentioned critical speed is definitely different from that classically understood and being related to the resonance of rotors undergoing excitation by an unbalanced inertia (Przybyłowicz, 1999b; Kurnik, 1988).

From the point of view of design of fast-rotating shafts, the critical speed (the dynamic instability threshold) is of the greatest importance. The critical threshold can be passively controlled, to some extent, by a suitable choice of structural parameters of the given shaft system. Equally important is the behaviour of the shaft in the neighbourhood of the critical point. The self-excited vibration can be of soft or hard character. In the first case the growth of the vibration amplitude is continuous, in the latter one exceeding of the criticality leads to a rapid jump of the amplitude. The phenomenon of the near-critical amplitude hysteresis is observed in that case.

The last several years have been characterised by an animated interest of scientific researchers and engineers in the so-called smart materials and structures that, in contradistinction to the classical ones, can adapt their properties to varying operating conditions according to the given algorithm. Smart systems combine mechanical properties with non- mechanical ones, most often with electric, magnetic, thermal, or sometimes optical fields of interaction. The most popular smart structures employ elements controllable by easy-to-transduce electric signals. Predominantly, piezoelectric elements made of lead zirconate titanate or polyvinylidene fluoride are applied.

The concept of piezoelectric stabilisation of rotating shafts was described by Przybyłowicz (1999b), who investigated the efficiency of making use of the bending action of piezoelements glued around the perimeter of the considered shaft. The idea of actuation was adopted from formerly elaborated approaches toward control of the bending modes in tubes and pipes with axi-symmetric cross-sections (Przybyłowicz, 1996). In the following papers the author puts

emphasis on the non-linear response of a rotating shaft with piezoelectric stabilisation system, as it occurred that the derived equations of motion contain coefficients corresponding to active control next to the non-linear terms, which do not vanish for zeroed bifurcation parameter, i.e. rotation speed, and which is the necessary condition of Hopf's theorem of the existence of a bifurcating solution, see Iooss and Joseph (1980), Kurnik (1988) and Przybyłowicz (1999a, 2000)

Recent developments in the field of smart structures and appearance of active composites have opened new possibilities to the control of rotating shafts. Composite shafts, due to low specific weight, anisotropic properties, and excellent torsional stiffness are very competitive materials with respect to their traditional steel counterparts. The application of active piezoelectric fibers makes them even more competitive. Main features of the piezoelectric fiber composite (PFC) shafts and the concept of their actuation was signalled by Przybyłowicz (2001a,b, 2002). The use of PFCs to rotating columns subject to follower loads and their efficient operation was confirmed by Kurnik and Przybyłowicz (2001, 2002).

In this paper, fundamentals of active control of rotating shafts made of smart laminates containing piezoelectric fibers will be given in detail. The theoretical grounds as well as earlier considerations on the criteria for designing optimal shaft structures by Kurnik (1995a,b) and Tylikowski (1980, 1993) will be very helpful in reaching this goal.

2. Constitutive equations of active composites with piezoelectric fibers

2.1. Introduction

The integration of piezoceramic (PZT) fibers within composite materials represents a new type of material evolution. Tiny PZT fibers of 30 μm in diameter can be aligned in an array, electrodized with interdigital electrodes and then integrated into planar architectures. Such architectures are embedded within glass or graphite fiber-reinforced polymers and become piezoelectric after being poled (Sporn and Schoencker, 1999). The idea of combining piezoceramics with polymers occurred in the 1980s (Newnham et al., 1980) and several years later it evolved towards smart composite materials. Piezoelectric Fiber Composites (PFCs) have a large potential for controlling. Matrix and ceramic combinations, volume fractions, and ply angles contribute to the tailorability

of PFCs (Bent et al., 1995), which make them applicable to structures requiring highly distributed actuation and sensing. Manufacturing technologies of PFCs have been adopted from graphite/epoxy manufacturing methods.

Composites with embedded active fibers are more resistant to damage and less obtrusive in active control. Active composites can essentially be formed from two types of piezoelectric fibers: short and long ones. Short-fiber composites have very high frequency response but generally produce low displacements. They are used for ultrasonic applications. On the other hand, long fibers can be used to create large sheets or lamina which produce extensional, bending and twisting motion of the composite. Such structures are suitable for low and mid-frequency vibration and acoustic control applications.

Looking for even more pronounced electromechanical efficiency of active composites, Xiang-Dong Chen et al. (1998) reported that special fabrication techniques and poling procedures considerably affect the final piezoelectric coefficients. They observed that appropriate solvent treatment in ceramic/polymer lamina increases the d_{33} constant by up to 5 times with respect to virgin specimens. Admittedly, their work dealt with PZT powder 3 μm particles sustained in a dielectric gel polymer (PVDF) instead of PZT fibers.

The integration of laminated composites with piezoelectric materials enjoys considerable practical interest. A study on the effect of stretching-bending coupling in PFC plates was investigated by Wang et al. (2000), who concentrated on the problem of proper placement of sensor/actuator pairs to achieve robust vibration control and avoid accidental instabilities. Control of coupled bending and twisting in PZT/epoxy laminas was discussed by Aldraihem and Wetherhold (1997). A shear-deformable beam theory was used by the authors to approximate the bending and twisting behaviour. By making use of FEM analysis they confirmed that the PZT/Ep layers rapidly and effectively suppress such a vibration mode in beam structures.

2.2. Theoretical grounds

Consider a single PFC lamina with piezoelectric fibers poled along the normal direction by manufacture as shown in Fig. 1.

In accordance with the constitutive equations of piezoelectricity (Nye, 1985; Damjanovič and Newnham, 1992), the stress-strain-electric field relation is

$$\varepsilon_i = s_{ij}\sigma_j + d_{ij}^{*\top} E_j \tag{2.1}$$

where ε_i denotes the strain, s_{ij} – compliance coefficients, d_{ij}^{*} – electromechanical coupling constants, E_j – electric field. Writting (2.1) explicitly

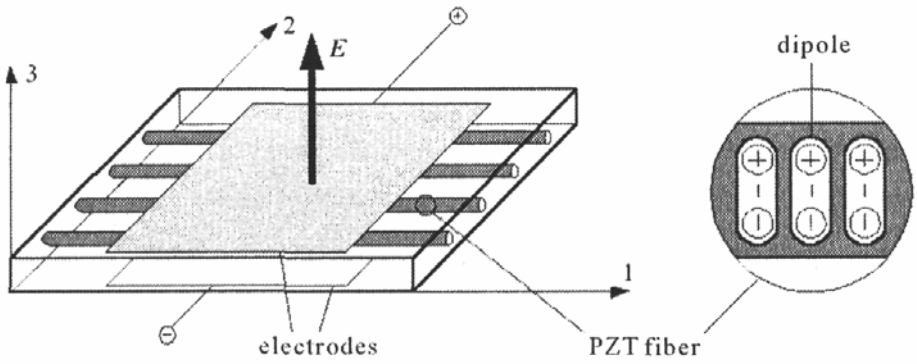

Fig. 1. Geometric configuration of active fibers and the poling direction

$$\begin{bmatrix} \varepsilon_1 \\ \varepsilon_2 \\ \varepsilon_3 \\ \varepsilon_4 \\ \varepsilon_5 \\ \varepsilon_6 \end{bmatrix} = \begin{bmatrix} s_{11} & s_{12} & s_{13} & 0 & 0 & 0 \\ s_{12} & s_{22} & s_{13} & 0 & 0 & 0 \\ s_{13} & s_{13} & s_{33} & 0 & 0 & 0 \\ 0 & 0 & 0 & s_{44} & 0 & 0 \\ 0 & 0 & 0 & 0 & s_{44} & 0 \\ 0 & 0 & 0 & 0 & 0 & s_{66} \end{bmatrix} \begin{bmatrix} \sigma_1 \\ \sigma_2 \\ \sigma_3 \\ \tau_4 \\ \tau_5 \\ \tau_6 \end{bmatrix} + \begin{bmatrix} 0 & 0 & d_{31}^* \\ 0 & 0 & d_{32}^* \\ 0 & 0 & d_{33}^* \\ 0 & d_{15}^* & 0 \\ d_{15}^* & 0 & 0 \\ 0 & 0 & 0 \end{bmatrix} \begin{bmatrix} E_1 \\ E_2 \\ E_3 \end{bmatrix} \tag{2.2}$$

where the form of the compliance matrix $\{s_{ij}\}$ as well as the electromechanical coupling $\{d_{ij}^*\}$ is typical for lead zirconate titanate (PZT) piezoceramics incorporated with active composites. The superscript "*" is used to emphasise that PZT elements operate together with a polymer matrix they are embedded into. In fact, pure PZTs exhibit the same effect in both perpendicular directions: $d_{31} = d_{32}$.

Naturally, equations (2.1), (2.2) describe a general case, in which the given active material can be used. As the considered single lamina undergoes an in-plane stress-strain state and, furthermore, the electric field is applied along the 3rd axis, equation (2.2) assumes a simpler form

$$\begin{bmatrix} \varepsilon_1 \\ \varepsilon_2 \\ \varepsilon_6 \end{bmatrix} = \begin{bmatrix} s_{11} & s_{12} & 0 \\ s_{12} & s_{22} & 0 \\ 0 & 0 & s_{66} \end{bmatrix} \begin{bmatrix} \sigma_1 \\ \sigma_2 \\ \tau_6 \end{bmatrix} + \begin{bmatrix} 0 & 0 & d_{31}^* \\ 0 & 0 & d_{32}^* \\ 0 & 0 & 0 \end{bmatrix} \begin{bmatrix} 0 \\ 0 \\ E_3 \end{bmatrix} \tag{2.3}$$

or simply

$$\boldsymbol{\varepsilon} = \mathbf{S}\boldsymbol{\sigma} + \mathbf{d}^* \boldsymbol{E} \tag{2.4}$$

where $s_{11} = 1/Y_1$, $s_{22} = 1/Y_2$, $s_{12} = -\nu_{12}/Y_1$, $s_{66} = 1/2G_{12}$ with Y_1, Y_2 being Young's moduli in the principal anisotropy axes 1, 2, G_{12} – Kirchhoff's modulus, and ν_{12} – Poisson's ratio. Transforming (2.3) in such a way so that

the stress vector $\boldsymbol{\sigma}$ could be expressed in terms of the mechanical strain $\boldsymbol{\varepsilon}$ and the electric field $\boldsymbol{E}$, one obtains

$$\boldsymbol{\sigma} = \mathbf{S}^{-1}\boldsymbol{\varepsilon} - \mathbf{S}^{-1}\mathbf{d}^{*\top}\boldsymbol{E} = \mathbf{Q}\boldsymbol{\varepsilon} - \mathbf{Q}\mathbf{d}^{*\top}\boldsymbol{E} = \mathbf{Q}\boldsymbol{\varepsilon} - \boldsymbol{\Xi}\boldsymbol{E} \tag{2.5}$$

where

$$\mathbf{Q} = \mathbf{S}^{-1} \qquad \boldsymbol{\Xi} = \mathbf{d}^{*\top}\boldsymbol{E} \tag{2.6}$$

or explicitly

$$\begin{bmatrix} \sigma_1 \\ \sigma_2 \\ \tau_6 \end{bmatrix} = \begin{bmatrix} Q_{11} & Q_{12} & 0 \\ Q_{12} & Q_{22} & 0 \\ 0 & 0 & Q_{66} \end{bmatrix} \begin{bmatrix} \varepsilon_1 \\ \varepsilon_2 \\ \gamma_6/2 \end{bmatrix} + \begin{bmatrix} 0 & 0 & \Xi_{13} \\ 0 & 0 & \Xi_{23} \\ 0 & 0 & 0 \end{bmatrix} \begin{bmatrix} 0 \\ 0 \\ E_3 \end{bmatrix} \tag{2.7}$$

where

$$\begin{aligned} Q_{11} &= \frac{Y_1}{1-\nu_{12}^2\frac{Y_2}{Y_1}} & Q_{22} &= \frac{Y_2}{1-\nu_{12}^2\frac{Y_2}{Y_1}} \\ Q_{12} &= \frac{\nu_{12}Y_2}{1-\nu_{12}^2\frac{Y_2}{Y_1}} & Q_{66} &= 2G_{12} \\ \Xi_{13} &= d_{31}^* Q_{11} + d_{32}^* Q_{12} & \Xi_{23} &= d_{31}^* Q_{12} + d_{32}^* Q_{22} \end{aligned} \tag{2.8}$$

Equations (2.3)-(2.8) describe the stress-strain-electric field state in the whole single PFC lamina, provided that the Young, Kirchhoff moduli and Poisson ratios are referred to the entire structure, i.e. the complex structure consisting of the matrix reinforced with e.g. glass or graphite mixed with PZT fibers. Approximate values of Y_1, Y_2, G_{12} and ν_{12} can be found in numerous papers on mechanical properties of composites, see e.g. Ashton et al. (1969), Jones (1975), Kurnik and Tylikowski (1997), or can be calculated from the rule of mixtures (Hahn, 1980). The same remark refers to the problem of finding the effective, say, equivalent electromechanical constants d_{ij}^* of the active piezoelectric material hosted by the matrix in an active composite. Fortunately, there is a lot of substantial information regarding this issue. Jiang and Batra (2002) discussed the equivalence energy principle to derive the effective thermo-elasto-mechanical properties of a four-phase composite consisting of an elastic matrix, shape memory alloy, piezoelectric and inert inclusions. They found that the inclusions highly affect the electromechanical coupling constants as well as they shift the stress threshold required to indicate the phase transformation in the SMA fibers. A three-phase model was earlier examined by Jiang and Cheung (2000) who developed a self-consistent approach for predicting the effective electro-elastic moduli of PFCs via a micromechanics model, see also Yu (1999).

2.3. Transformation of the constitutive equations

Apply now an active lamina, the principal anisotropy axes of which (1,2) are skewed by the angle θ with respect to the main axes (x, y) of the given host structure, see Fig. 2. The main matrix operator corresponding to such a transformation contains cosines of angles between the axes of the original and rotated co-ordinate system. Denoting the stress and strain vectors in the new co-ordinate system by $\overline{\boldsymbol{\sigma}} = [\sigma_x, \sigma_y, \tau_{xy}]$ and $\overline{\boldsymbol{\varepsilon}} = [\varepsilon_x, \varepsilon_y, \gamma_{xy}/2]$, respectively (the overbars mean relative to the rotated system), one writes down

$$\overline{\boldsymbol{\sigma}} = \overline{\mathbf{Q}}\overline{\boldsymbol{\varepsilon}} - \overline{\boldsymbol{\Xi}}\overline{\boldsymbol{E}} \tag{2.9}$$

where, in fact, $\overline{\boldsymbol{E}} = \boldsymbol{E}$ (the electric field is applied along the 3rd axis, which remains unchanged during transformation: $z \equiv 3$).

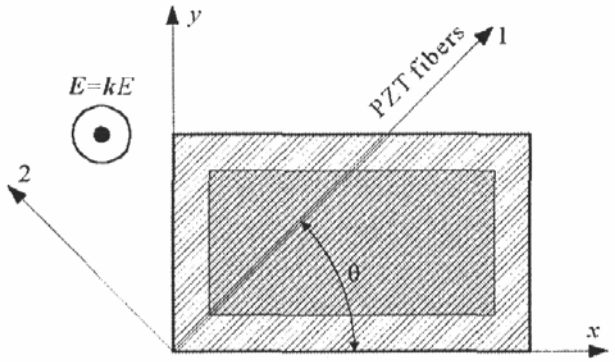

Fig. 2. Rotation of the co-ordinate system $(1, 2) \rightarrow (x, y)$ by θ

In order to find the transformed matrices $\overline{\mathbf{Q}}$ and $\overline{\boldsymbol{\Xi}}$, one incorporates the formula for transforming tensors via rotation

$$Q_{kl} = Q_{ij}\alpha_{ik}\alpha_{jl} \tag{2.10}$$

where $\alpha_{mn} = \cos\angle(\boldsymbol{e}_m, \boldsymbol{h}_n)$ and where $\boldsymbol{e}_m$ is the mth base vector of the original co-ordinate system, and $\boldsymbol{h}_n$ – the nth base vector in the rotated system. Substituting $\sigma_x = \overline{\sigma}_{11}$, $\sigma_y = \overline{\sigma}_{22}$, $\tau_{xy} = \overline{\sigma}_{12}$ and $\varepsilon_x = \overline{\varepsilon}_{11}$, $\varepsilon_y = \overline{\varepsilon}_{22}$, $\gamma_{xy} = 2\overline{\varepsilon}_{12}$ into (2.10) one obtains

$$\begin{bmatrix} \sigma_x \\ \sigma_y \\ \tau_{xy} \end{bmatrix} = \begin{bmatrix} \cos^2\theta & \sin^2\theta & \sin 2\theta \\ \sin^2\theta & \cos^2\theta & -\sin 2\theta \\ -\dfrac{1}{2}\sin 2\theta & \dfrac{1}{2}\sin 2\theta & \cos 2\theta \end{bmatrix} \begin{bmatrix} \sigma_1 \\ \sigma_2 \\ \sigma_{12} \end{bmatrix} = \mathbf{T} \begin{bmatrix} \sigma_1 \\ \sigma_2 \\ \sigma_{12} \end{bmatrix} \tag{2.11}$$

and

$$\begin{bmatrix} \varepsilon_x \\ \varepsilon_y \\ \frac{1}{2}\gamma_{xy} \end{bmatrix} = \mathbf{T} \begin{bmatrix} \varepsilon_1 \\ \varepsilon_2 \\ \frac{1}{2}\gamma_{12} \end{bmatrix} \tag{2.12}$$

In that case the stiffness matrix contains no more the zero coefficients

$$\overline{\mathbf{Q}} = \mathbf{T}\mathbf{Q}\mathbf{T}^{-1} = \begin{bmatrix} \overline{Q}_{11} & \overline{Q}_{12} & \overline{Q}_{16} \\ \overline{Q}_{12} & \overline{Q}_{22} & \overline{Q}_{26} \\ \overline{Q}_{16} & \overline{Q}_{26} & \overline{Q}_{66} \end{bmatrix} \tag{2.13}$$

where the coefficients $\overline{Q}_{ij} = \overline{Q}_{ij}(\theta)$ are explicitly given in the paper by Kurnik and Tylikowski (1997) or Ashton et al. (1969). The new form of the transformed electromechanical coupling matrix $\overline{\boldsymbol{\Xi}}$ is

$$\overline{\boldsymbol{\Xi}} = \mathbf{T}\overline{\boldsymbol{\Xi}} = \mathbf{T}\mathbf{Q}\mathbf{d}^* = \begin{bmatrix} 0 & 0 & \overline{\Xi}_{13} \\ 0 & 0 & \overline{\Xi}_{23} \\ 0 & 0 & \overline{\Xi}_{33} \end{bmatrix} \tag{2.14}$$

where

$$\begin{aligned} \overline{\Xi}_{13} &= \Xi_{13}\cos^2\theta + \Xi_{23}\sin^2\theta \\ \overline{\Xi}_{23} &= \Xi_{13}\sin^2\theta + \Xi_{23}\cos^2\theta \\ \overline{\Xi}_{33} &= \frac{1}{2}(\Xi_{23} - \Xi_{13})\sin 2\theta \end{aligned} \tag{2.15}$$

2.4. Constitutive equations of an active laminate structure

Derive now the constitutive equations for laminated panels with active piezoelectric fibers based on Mindlin's assumption of constant transverse displacement along the plate thickness, where the strain-displacement relations (first order deformation theory) are given by

$$\begin{aligned} \varepsilon_x &= \frac{\partial u_0}{\partial x} - z\frac{\partial^2 w_0}{\partial x^2} = \varepsilon_{x0} + z\kappa_x \\ \varepsilon_y &= \frac{\partial v_0}{\partial y} - z\frac{\partial^2 w_0}{\partial y^2} = \varepsilon_{y0} + z\kappa_y \\ \gamma_{xy} &= \frac{\partial v_0}{\partial x} + \frac{\partial u_0}{\partial y} - 2z\frac{\partial^2 w_0}{\partial x \partial y} = \gamma_{xy0} + 2z\kappa_{xy} \end{aligned} \tag{2.16}$$

or simply

$$\boldsymbol{\varepsilon} = \boldsymbol{\varepsilon}_0 + z\boldsymbol{\kappa} \tag{2.17}$$

where ε_x, ε_y, γ_{xy} denote the longitudinal strains in the x, y directions and the shear strain, respectively, z is the co-ordinate measured through the thickness of the panel, u and v – longitudinal displacements in the x and y directions, respectively, κ_x and κ_y – curvatures with respect to the x and y, and κ_{xy} is related to torsional displacement. The index "0" refers to the middle surface of the panel. The transverse displacement is denoted by w (w_0).

Find now the internal forces and moments acting per unit length in a N-layer laminate

$$\boldsymbol{N} = \int_{h_1}^{h_2} \overline{\boldsymbol{\sigma}}\, dz = \sum_{k=1}^{N} \int_{z_{k-1}}^{z_k} (\overline{\mathbf{Q}}_k \overline{\boldsymbol{\varepsilon}}_k - \overline{\boldsymbol{\Xi}}_k \boldsymbol{E}_k)\, dz \tag{2.18}$$

where k is the layer number. Substitution of (2.16) into (2.18) yields

$$\boldsymbol{N} = \boldsymbol{\varepsilon}_0 \sum_{k=1}^{N} \overline{\mathbf{Q}}_k (z_k - z_{k-1}) + \frac{1}{2}\boldsymbol{\kappa} \sum_{k=1}^{N} \overline{\mathbf{Q}}_k (z_k^2 - z_{k-1}^2) - \sum_{k=1}^{N} \overline{\boldsymbol{\Xi}}_k \boldsymbol{E}_k (z_k - z_{k-1}) \tag{2.19}$$

where

$$\begin{aligned} &\overline{\boldsymbol{\varepsilon}}_k = \left[\varepsilon_x, \varepsilon_y, \frac{1}{2}\gamma_{xy}\right] \qquad\qquad \boldsymbol{N} = [N_x, N_y, N_{xy}] \\ &\overline{\boldsymbol{\varepsilon}}_0 = \left[\varepsilon_{x0}, \varepsilon_{y0}, \frac{1}{2}\gamma_{xy0}\right] \\ &\boldsymbol{\kappa} = \left[-\frac{\partial^2 w_0}{\partial x^2}, -\frac{\partial^2 w_0}{\partial y^2}, -2\frac{\partial^2 w_0}{\partial x \partial y}\right] \end{aligned} \tag{2.20}$$

Proceeding in a similar way one determines the moments

$$\boldsymbol{M} = \int_{h_1}^{h_2} \overline{\boldsymbol{\sigma}} z\, dz = \sum_{k=1}^{N} \int_{z_{k-1}}^{z_k} z(\overline{\mathbf{Q}}_k \overline{\boldsymbol{\varepsilon}}_k - \overline{\boldsymbol{\Xi}}_k \boldsymbol{E}_k)\, dz \tag{2.21}$$

which, after some transformations, assume the form

$$\boldsymbol{M} = \frac{1}{2}\boldsymbol{\varepsilon}_0 \sum_{k=1}^{N} \overline{\mathbf{Q}}_k (z_k^2 - z_{k-1}^2) + \frac{1}{3}\boldsymbol{\kappa} \sum_{k=1}^{N} \overline{\mathbf{Q}}_k (z_k^3 - z_{k-1}^3) - \frac{1}{2} \sum_{k=1}^{N} \overline{\boldsymbol{\Xi}}_k \boldsymbol{E}_k (z_k^2 - z_{k-1}^2) \tag{2.22}$$

By denoting

$$\begin{aligned} &\mathbf{A} = \sum_{k=1}^{N} \overline{\mathbf{Q}}_k (z_k - z_{k-1}) \qquad\qquad \mathbf{B} = \frac{1}{2} \sum_{k=1}^{N} \overline{\mathbf{Q}}_k (z_k^2 - z_{k-1}^2) \\ &\mathbf{D} = \frac{1}{3} \sum_{k=1}^{N} \overline{\mathbf{Q}}_k (z_k^3 - z_{k-1}^3) \end{aligned} \tag{2.23}$$

and

$$\begin{aligned} \boldsymbol{N}^A &= \sum_{k=1}^{N} \overline{\Xi}_k \boldsymbol{E}_k (z_k - z_{k-1}) \qquad \text{or} \qquad \boldsymbol{N}^A = \textstyle\sum_{k=1}^{N} \overline{\Xi}_k^{(S)} \boldsymbol{E}_k (z_k - z_{k-1}) \\ \boldsymbol{M}^A &= \tfrac{1}{2} \textstyle\sum_{k=1}^{N} \overline{\Xi}_k \boldsymbol{E}_k (z_k^2 - z_{k-1}^2) \qquad \text{or} \qquad \boldsymbol{M}^A = \tfrac{1}{2} \textstyle\sum_{k=1}^{N} \overline{\Xi}_k^{(S)} \boldsymbol{E}_k (z_k^2 - z_{k-1}^2) \end{aligned} \tag{2.24}$$

one finally obtains the constitutive equations for the active laminate structure

$$\begin{bmatrix} \boldsymbol{N} \\ \boldsymbol{M} \end{bmatrix} = \begin{bmatrix} \mathsf{A} & \mathsf{B} \\ \mathsf{B} & \mathsf{D} \end{bmatrix} \begin{bmatrix} \boldsymbol{\varepsilon}_0 \\ \boldsymbol{\kappa} \end{bmatrix} - \begin{bmatrix} \boldsymbol{N}^A \\ \boldsymbol{M}^A \end{bmatrix} \tag{2.25}$$

3. Simplified theory of bending in an active composite shaft

In the following considerations the state of loading and displacement of a thin-walled cylindrical laminated shell will be assumed in such way that the deflection of the geometric axis remains plane. Neglecting the effect of shear strains and assuming Kirchhoff's and Mindlin's simplifications one can consider the balance of internal forces and moments, see Fig. 3, in order to obtain equations of transverse motion of the shaft element.

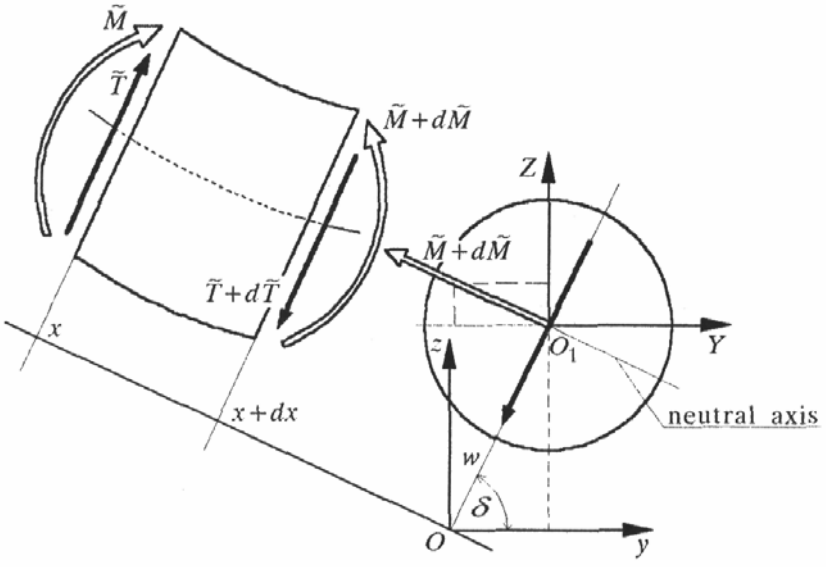

Fig. 3. Bending moments and transverse forces acting on an infinitesimal element of the shaft

These equations are

$$\rho A\frac{\partial^2 y}{\partial t^2} = -\frac{\partial \widetilde{T}}{\partial x}\cos\delta$$
$$\rho A\frac{\partial^2 z}{\partial t^2} = -\frac{\partial \widetilde{T}}{\partial x}\sin\delta + q \tag{3.1}$$

where ρ is the mass density of the laminate, A – cross-sectional area, y, z – transverse co-ordinates, $\widetilde{T}$ – transverse force, δ – angular position of the plane of bending, q – external load per unit length. By balancing the moments one concludes

$$\widetilde{T} = \frac{\partial \widetilde{M}}{\partial x} = \frac{\partial}{\partial x}(M + M^A) \tag{3.2}$$

where the tildes refer to total quantities, i.e. the sums of internal forces and moments resulting from pure mechanical shear and bending, plus the respective values coming from action of piezoelectric fibers, hence: $\widetilde{M} = M + M^A$ and $\widetilde{T} = T + T^A$.

Now, the most important task is finding an explicit formula for the bending moment $\widetilde{M}$. Like in the work by Kurnik and Tylikowski (1997), Bauchau's (1980) simplifications will be assumed. They are as follows:

- the elements A_{16} and A_{26} of the stiffness matrix are negligible (which is true for a greater number of layers in symmetric composites). In anti-symmetric structures A_{16}, A_{26} are always zero;
- couplings between curvatures κ_x, κ_y, κ_{xy} and internal forces N_x, N_y and N_{xy} are omitted. This is always true for symmetric laminates, and admissible in anti- symmetric ones with numerous layers;
- perpendicular component y can be neglected with respect to the tensile force N_x during bending along the x-axis (by M_x).

By applying the above assumptions to the constitutive equations of an active composite (2.25) one obtains

$$N_x = A_{11}\varepsilon_{x0} + A_{12}\varepsilon_{y0} - N_x^A$$
$$0 = A_{12}\varepsilon_{x0} + A_{22}\varepsilon_{y0} - N_y^A \tag{3.3}$$

what yields

$$N_x = \Big(A_{11} - \frac{A_{12}^2}{A_{22}}\Big)\varepsilon_{x0} + N_x^A - N_y^A\frac{A_{12}}{A_{22}} \tag{3.4}$$

Although the energy dissipation due to application of active elements and an appropriate control strategy are the key factors for further considerations, the internal damping resulting from natural properties of laminates is a very important problem which cannot be disregarded.

Assuming a simple rheological model of a single lamina, e.g. Kelvin-Voigt's one, the Young and Kirchhoff moduli get operational forms

$$\begin{aligned} Y_i^* &= Y_i\Big(1+\beta_i\frac{\partial}{\partial t}\Big) \qquad i=1,2 \\ G_{12}^* &= G_{12}\Big(1+\beta_{12}\frac{\partial}{\partial t}\Big) \end{aligned} \tag{3.5}$$

Taking into account that, predominantly, $Y_2 \ll Y_1$, one finds that all elasticity constants in a transformed (rotated) co-ordinate system have a similar first-order (K-V-like) form

$$\overline{Q}_{ij}^* = \overline{Q}_{ij} + \overline{Q}_{ij}^{\beta}\frac{\partial}{\partial t} \tag{3.6}$$

where $\overline{Q}_{ij} = \overline{Q}_{ij}(..., Q_{kl}, ..., \theta)$ and $\overline{Q}_{ij}^{\beta} = \overline{Q}_{ij}(..., Q_{kl}, ..., \beta_{kl}, ..., \theta)$. Explicitly, the operational Young modulus of the entire laminate is

$$Y_B^* = Y_B\frac{1+\beta_1\frac{\partial}{\partial t}+\beta_2\frac{\partial^2}{\partial t^2}}{1+c\frac{\partial}{\partial t}} \tag{3.7}$$

where

$$\begin{aligned} Y_B &= \frac{\overline{Q}_{11}\overline{Q}_{22}-\overline{Q}_{12}^2}{\overline{Q}_{22}} \qquad & \beta_1 &= \frac{\overline{Q}_{11}\overline{Q}_{22}^{\beta}+\overline{Q}_{22}\overline{Q}_{11}^{\beta}-2\overline{Q}_{12}\overline{Q}_{12}^{\beta}}{\overline{Q}_{11}\overline{Q}_{22}-\overline{Q}_{12}^2} \\ \beta_2 &= \frac{\overline{Q}_{11}^{\beta}\overline{Q}_{22}^{\beta}-(\overline{Q}_{12}^{\beta})^2}{\overline{Q}_{11}\overline{Q}_{22}-\overline{Q}_{12}^2}, & c &= \frac{\overline{Q}_{12}^{\beta}}{\overline{Q}_{12}} \end{aligned} \tag{3.8}$$

and where

$$\begin{aligned} \overline{Q}_{11}^{\beta} &= \beta_{11}Q_{11}\cos^4\theta+\beta_{22}Q_{22}\sin^4\theta+\Big(\beta_{12}Q_{66}+\frac{1}{2}\beta_{22}Q_{12}\Big)\sin^2 2\theta \\ \overline{Q}_{22}^{\beta} &= \beta_{11}Q_{11}\sin^4\theta+\beta_{22}Q_{22}\cos^4\theta+\Big(\beta_{12}Q_{66}+\frac{1}{2}\beta_{22}Q_{12}\Big)\sin^2 2\theta \\ \overline{Q}_{12}^{\beta} &= \Big(\frac{1}{4}\beta_{11}Q_{11}+\beta_{12}Q_{66}+\frac{1}{4}\beta_{22}Q_{22}\Big)\sin^2 2\theta+\frac{Q_{12}}{4}\beta_{22}(3+\cos 4\theta) \end{aligned} \tag{3.9}$$

For further simplification of (3.7), i.e. for finding a local K-V model of the entire structure, the operator Y_B^* is expanded into Taylor's series with $\partial/\partial t$

replaced with $i\omega$ just before. This should be done in the neighbourhood of a chosen frequency, say, the first eigenfrequency ω_{I} – a characteristic one, probably close to the expected frequency of self-excited vibration the control system is made to fight against. All of that implies the following local and equivalent operational Young's modulus

$$Y_B^* = Y_0\Big(1 + \beta_0 \frac{\partial}{\partial t}\Big) \tag{3.10}$$

where

$$\begin{aligned} Y_0 &= Y_B \frac{1 + 2c\omega_{\mathrm{I}} + (\beta_1 c - \beta_2)\omega_{\mathrm{I}}^2}{(1 + c\omega_{\mathrm{I}})^2} \\ \beta_0 &= \frac{\beta_1 - c + \omega_{\mathrm{I}}\beta_2(2 + c\omega_{\mathrm{I}})}{1 + 2c\omega_{\mathrm{I}} + (\beta_1 c - \beta_2)\omega_{\mathrm{I}}^2} \qquad \omega_{\mathrm{I}} = \frac{\pi^2}{l^2}\sqrt{\frac{Y_B J}{\rho A}} \end{aligned} \tag{3.11}$$

where J and l are the geometric cross-sectional moment of inertia and length of the shaft, respectively.

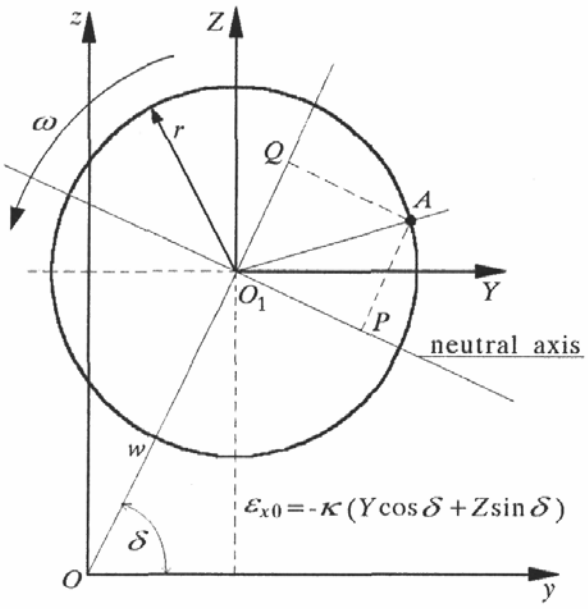

Fig. 4. Tensile strain at an arbitrary point of the shaft cross-section

Return now to the question of bending moment in order to close the equations of motion. To this end, consider the tensile strain at a given point fixed on the midsurface, see Fig. 4. Taking into account the ovalisation effect of the circular cross-section under bending, i.e. the so-called Brazier's effect, see

Kurnik (1993), Birman and Bert (1987) as well as Reisner (1959), one writes down

$$\varepsilon_{x0} = -\kappa(1-\gamma\kappa^2)(Y\cos\delta + Z\sin\delta) \tag{3.12}$$

where the coefficient of the ovalisation is

$$\gamma = \frac{3r^4 Y_0}{2Q_{22}h^2 + 8r^4\rho\omega^2} \tag{3.13}$$

Furthermore, regarding moderate deflections of the shaft axis during transverse motion, i.e. the first non-linear approximation of the curvature κ

$$\kappa = \frac{\frac{\partial^2 w}{\partial x^2}}{\sqrt{\left[1+\left(\frac{\partial w}{\partial x}\right)^2\right]^3}} \approx \frac{\partial^2 w}{\partial x^2}\left[1-\frac{3}{2}\left(\frac{\partial w}{\partial x}\right)^2\right] \tag{3.14}$$

the strain will be

$$\varepsilon_{x0} = -\left(Y\frac{\partial^2 y}{\partial x^2} + Z\frac{\partial^2 z}{\partial x^2}\right)\left\{1-\frac{3}{2}\left[\left(\frac{\partial y}{\partial x}\right)^2 + \left(\frac{\partial z}{\partial x}\right)^2\right] - \gamma\left[\left(\frac{\partial^2 y}{\partial x^2}\right)^2 + \left(\frac{\partial^2 z}{\partial x^2}\right)^2\right]\right\} \tag{3.15}$$

as $y = w\cos\delta$ and $z = w\sin\delta$, see Fig. 4. The purely mechanical component M of the bending moment $\widetilde{M}$ ($\widetilde{M} = M + M^A$) is

$$\boldsymbol{M} = \begin{bmatrix} M_y \\ M_z \end{bmatrix} = \int\limits_A \begin{bmatrix} Z \\ Y \end{bmatrix} \sigma_x \, dA = \int\limits_A \begin{bmatrix} Z \\ Y \end{bmatrix} \left(1+\beta_0\frac{\partial}{\partial t}\right)\varepsilon_{x0} \, dA \tag{3.16}$$

where it should be taken into account that: $\dot{Y} = -\omega Z$, $\dot{Z} = \omega Y$, $\int_A YZ\, dA = 0$ and $\int_A Y^2\, dA = \int_A Z^2\, dA = J$.

4. Actuation of the rotating shaft

In this section the problem of actuation in a rotating shaft is to be analysed. Consider a single layer of a composite shaft with an electrode covering a single bunch of piezoelectric fibers embedded right beneath the electrode, see Fig. 5.

The bending moment M_{ij}^A produced by the jth actuator in the ith composite layer is

$$M_{ij}^A = \int\limits_{A_{ij}} \sigma_x^A PS\, dA = \int\limits_{A_{ij}} \Xi_\sigma E_{ij} r\sin\varphi \, dA \tag{4.1}$$

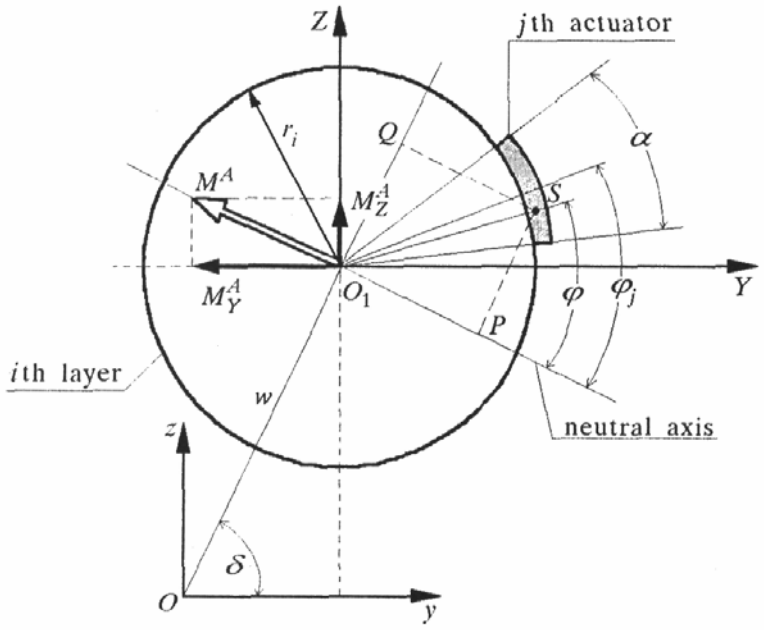

Fig. 5. Actuator patch controlling a part of piezoelectric fibers

where E_{ij} is the electric field applied to the jth electrode on the ith layer, and $\Xi_\sigma = \overline{\Xi}_{13} - \overline{\Xi}_{23}\overline{Q}_{12}/\overline{\Xi}_{22}$. The integration area A_{ij} appearing in (4.1) can be described as follow

$$A_{ij} = \left\{(r,\varphi): \quad r_i \leqslant r \leqslant r_i + \frac{h}{N}, \quad \varphi_j - \frac{\alpha}{2} \leqslant \varphi \leqslant \varphi_j + \frac{\alpha}{2}\right\} \tag{4.2}$$

where r_i is the inside radius of the ith layer, h-thickness of the laminate shaft, N – number of layers, φ_j – current angular position of the middle point of the jth electrode patch (actuator), α – angular width of the electrode (assumed to be the same for every actuator). Hence

$$M^A_{ij} = \Xi_\sigma E_{ij} \int_{r_i}^{r_i+\frac{h}{N}} r^2\, dr \int_{\varphi_j-\frac{\alpha}{2}}^{\varphi_j+\frac{\alpha}{2}} \sin\varphi\, d\varphi \tag{4.3}$$

if the electric field and composition of the embedded piezoelectric fibers are homogeneous. Assuming that $h/r \ll 1$

$$M^A_{ij} = 2\Xi_\sigma E_{ij} r_i^2 \frac{h}{N} \sin\varphi_j \sin\frac{\alpha}{2} \tag{4.4}$$

According to the law of an ideal piezoelectric sensor (i.e. having negligible width), the measured voltage is directly proportional to the slope of the shaft

axis at the point x_s where the sensor ring is glued to the shaft surface

$$U_{Sij} = \Delta_1 \frac{h_s}{\epsilon_s} \frac{\partial^2 w(x_s)}{\partial x^2} r_i \sin\varphi_j$$
$$\Delta_1 = \frac{Y_s}{1-\nu_{s12}^2}[\sin^2\theta_s(d_{s32}+\nu_{s12}d_{s31}) + \cos^2\theta_s(d_{s31}+\nu_{s12}d_{s32})] \tag{4.5}$$

where θ_s is the angle through which the main anisotropy axes of the sensor are rotated with respect to the axis of the host structure, ϵ_s is the dielectric permittivity, ν_{s12} – Poisson's ratio, Y_s – Young's modulus, d_{s32} and d_{s31} electromechanical coupling constants of the sensor material.

Assuming a control strategy as a combination of the proportional and velocity feedback, one puts down

$$U_{Aij} = c_p U_{Sij} + c_d \frac{dU_{Sij}}{dt} \tag{4.6}$$

Knowing that $E_{ij} = U_{Aij}/(h/N)$ and $d\sin\varphi_j/dt = \omega\cos\varphi_j$, the electric field controlling the ijth actuator will be

$$E_{ij} = \frac{N\Delta_1 r_i h_s}{h\epsilon_s}\Big[c_p \frac{\partial^2 w(x_s,t)}{\partial x^2}\sin\varphi_j + c_d \frac{d}{dt}\Big(\frac{\partial^2 w(x_s,t)}{\partial x^2}\sin\varphi_j\Big)\Big] \tag{4.7}$$

and, finally, the actuating moment

$$M_{ij}^A = 2\Xi_\sigma \frac{\Delta_1 r_i^3 h_s}{\epsilon_s}\sin\varphi_j \sin\frac{\alpha}{2}\cdot$$
$$\cdot\ \Big[\Big(c_p\frac{\partial^2 w(x_s,t)}{\partial x^2} + c_d\frac{\partial^3 w(x_s,t)}{\partial x^2\partial t}\Big)\sin\varphi_j + c_d\omega\frac{\partial^2 w(x_s,t)}{\partial x^2}\cos\varphi_j\Big] \tag{4.8}$$

The resultant moment is

$$M^A = \sum_{i=1}^{N}\sum_{j=1}^{n} M_{ij}^A \tag{4.9}$$

where N is the number of layers the composite shaft is made of, n – number of electrode patches (actuators) along the perimeter of a single layer. Hence

$$M_{ij}^A = 2\Xi_\sigma \frac{\Delta_1 r_i^3 h_s}{\epsilon_s}\sin\frac{\alpha}{2}\Big[\Big(c_p\frac{\partial^2 w(x_s,t)}{\partial x^2} + c_d\frac{\partial^3 w(x_s,t)}{\partial x^2\partial t}\Big)\sum_{i=1}^{N} r_i^3 \sum_{j=1}^{n}\sin^2\varphi_j +$$
$$+\ c_d\omega\frac{\partial^2 w(x_s,t)}{\partial x^2}\sum_{i=1}^{N} r_i^3 \sum_{j=1}^{n}\sin\varphi_j\cos\varphi_j\Big] \tag{4.10}$$

Let r denote the average radius of the thin-walled shaft structure, thus

$$r_i = r + h\frac{2i-N}{N} = r\Big[1 + \frac{h}{2rN}(2i-N)\Big] \tag{4.11}$$

Since $h/r \ll 1$ (and additionally divided by $2N > 1$) it is reasonable to assume $r_i = r$, which entails

$$\sum_{i=1}^{N}\Big(r + h\frac{2i-N}{N}\Big)^3 \approx Nr^3 \tag{4.12}$$

Have a closer look now at the sums in (4.10) involving the expressions of the angular position φ_j. Note, that the angular distance between the jth and $(j+1)$th electrode patch is $\varphi_{j+1} - \varphi_j = 2\pi/n$. Denoting the position of the first patch by $\varphi_1 = \varphi$ one finds the locations of the subsequent electrodes to be: $\varphi_j = \varphi + 2\pi j/n$. Studying the properties of the sums in (4.10) one states

$$\sum_{j=1}^{n}\sin^2\varphi_j = \sum_{j=1}^{n}\sin^2\Big(\varphi_j + j\frac{2\pi}{n}\Big) = \begin{cases} \sin^2\varphi & \text{for} \quad n=1 \\ 2\sin^2\varphi & \text{for} \quad n=2 \\ \dfrac{n}{2} & \text{for} \quad n \geqslant 3 \end{cases} \tag{4.13}$$

and

$$\sum_{j=1}^{n}\sin\varphi_j\cos\varphi_j = \frac{1}{2}\sum_{j=1}^{n}\sin 2\Big(\varphi_j + j\frac{2\pi}{n}\Big) = \begin{cases} \dfrac{1}{2}\sin 2\varphi & \text{for} \quad n=1 \\ \sin 2\varphi & \text{for} \quad n=2 \\ 0 & \text{for} \quad n \geqslant 3 \end{cases} \tag{4.14}$$

It is a very important conclusion that the application of 3 or more electrode patches ensures generation of a constant bending moment, i.e. a non-pulsating one, despite the discrete distribution of the patches along the perimeter and rotary motion of the shaft. Finally

$$M^A = \Xi_\sigma \frac{N\Delta_1 r_i^3 h_s}{\epsilon_s}\Big(c_p\frac{\partial^2 w(x_s,t)}{\partial x^2} + c_d\frac{\partial^3 w(x_s,t)}{\partial x^2\partial t}\Big)n\sin\frac{\pi}{n} \tag{4.15}$$

where $\sin(\alpha/2)$ has been replaced with $\sin(\pi/n)$, which holds true for negligible gaps separating and insulating the electrode patches.

Except for the material and structural parameters, the actuating moment is directly proportional to the curvature and its first time derivative. There yet appears another parameter responsible for the magnitude of M^A – the

number n of the actuator electrodes per each layer. The question is to what extent M^A depends on n (what is the limit value of M^A, what is the minimum one?). To answer this, draw a diagram of the function $n\sin(\pi/n)$ standing in (4.15). The moment M^A is proportional to this function, see Fig. 6.

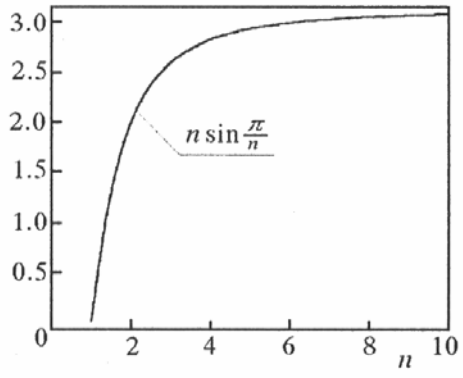

Fig. 6. Actuating moment vs. number of electrode patches

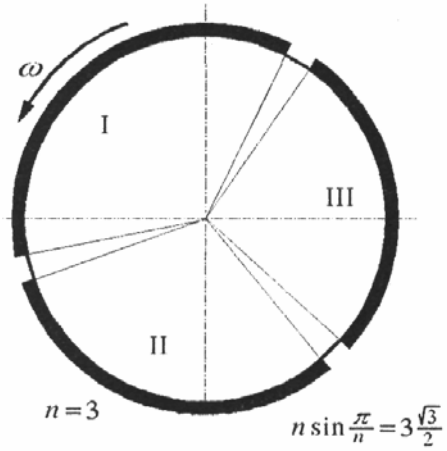

Fig. 7. The least number of electrodes generating a constant bending moment

The maximum bending moment produced by the piezoelectric fibers is strictly related with the following limit

$$\lim_{n\to\infty} n\sin\frac{\pi}{n} = \pi \tag{4.16}$$

It is clearly seen (Fig. 6) that infinite increasing of the number of electrode patches is useless. A fine segmentation of the electrodes yields results incommensurable with the degree of unavoidable technical complication of the control system. It is rather recommended to use possibly the least number of the actuators along the perimeter in achieving the desired effect, i.e. smooth operation of the stabilising system (constant counter-bending). This amounts to incorporation of a 3-electrode control set, see Fig. 7.

5. Equations of motion

Having derived the resultant bending moment generated by the active piezoelectric fibers, see (4.16), one substitutes it into (3.2) and then (3.1). Before doing this, notice however that (4.15) applies to the moment calculated with respect to the neutral bending axis. It has to be then decomposed into the y- and z-elements. Knowing that $y = w\cos\delta$ and $z = w\sin\delta$ (see Fig. 3) and $M_y^A = M^A\sin\delta$, $M_z^A = M^A\cos\delta$, one finds

$$\begin{bmatrix} M_y^A \\ M_z^A \end{bmatrix} = \left(k_p \begin{bmatrix} \dfrac{\partial^2 z(x_s,t)}{\partial x^2} \\ \dfrac{\partial^2 y(x_s,t)}{\partial x^2} \end{bmatrix} + k_d \begin{bmatrix} \dfrac{\partial^3 z(x_s,t)}{\partial x^2 \partial t} \\ \dfrac{\partial^3 y(x_s,t)}{\partial x^2 \partial t} \end{bmatrix} \right) \Big\{ H(x-x_1) - H(x-x_2) \Big\} \tag{5.1}$$

where

$$\begin{bmatrix} k_p \\ k_d \end{bmatrix} = \frac{3\sqrt{3}}{2}\Xi_\sigma \frac{N\Delta_1 h_s r^3}{\epsilon_s} \begin{bmatrix} c_p \\ c_d \end{bmatrix} \tag{5.2}$$

The presence of Heaviside's step functions $H(\cdot)$ results from the fact that the electrodes may not necessarily cover the entire length of the shaft, but only a part of it, e.g. between $x = x_1$ and $x = x_2$. Substituting (5.1) into (3.2) and (3.1) yields (in a dimensionless form)

$$\begin{aligned}
&\rho A\frac{\partial^2 y}{\partial t^2} + \eta\frac{\partial y}{\partial t} + Y_0 J\left\{ \frac{\partial^4 y}{\partial x^4}\Big\{1 - 2\Big(\frac{\partial y}{\partial x}\Big)^2 - \frac{3}{2}\Big(\frac{\partial z}{\partial x}\Big)^2 - \right. \\
&-3\beta_0\Big(\frac{\partial y}{\partial x}\frac{\partial^2 y}{\partial x\partial t} + \frac{\partial z}{\partial x}\frac{\partial^2 z}{\partial x\partial t}\Big) - \gamma\Big[3\Big(\frac{\partial^2 y}{\partial x^2}\Big)^2 + \Big(\frac{\partial^2 z}{\partial x^2}\Big)^2\Big] - \\
&\left. -2\beta_0\gamma\Big(\frac{\partial^2 z}{\partial x^2}\frac{\partial^3 z}{\partial x^2\partial t} + 3\frac{\partial^2 y}{\partial x^2}\frac{\partial^3 y}{\partial x^2\partial t} + \omega\frac{\partial^2 y}{\partial x^2}\frac{\partial^2 z}{\partial x^2}\Big)\Big\} + \right. \\
&+\beta_0\frac{\partial^5 y}{\partial x^4\partial t}\Big\{1 - 2\Big(\frac{\partial y}{\partial x}\Big)^2 - \frac{3}{2}\Big(\frac{\partial z}{\partial x}\Big)^2 - 3\gamma\Big[\Big(\frac{\partial^2 y}{\partial x^2}\Big)^2 + \Big(\frac{\partial^2 z}{\partial x^2}\Big)^2\Big]\Big\} + \\
&+\beta_0\omega\left\{ \frac{\partial^4 z}{\partial x^4}\Big\{1 - 2\Big(\frac{\partial y}{\partial x}\Big)^2 - \frac{3}{2}\Big(\frac{\partial z}{\partial x}\Big)^2 - \gamma\Big[\Big(\frac{\partial^2 y}{\partial x^2}\Big)^2 + 3\Big(\frac{\partial^2 z}{\partial x^2}\Big)^2\Big]\Big\} - \right. \\
&-3\Big(\frac{\partial^2 y}{\partial x^2}\Big)^2\frac{\partial^2 z}{\partial x^2} - \frac{\partial^2 y}{\partial x^2}\frac{\partial^3 z}{\partial x^3}\Big(7\frac{\partial y}{\partial x} + 4\gamma\frac{\partial^3 y}{\partial x^3}\Big) - \\
&\left. -\frac{\partial^2 z}{\partial x^2}\Big\{3\frac{\partial y}{\partial x}\frac{\partial^3 y}{\partial x^3} + 9\frac{\partial z}{\partial x}\frac{\partial^3 z}{\partial x^3} + 2\gamma\Big[\Big(\frac{\partial^3 y}{\partial x^3}\Big)^2 + 3\Big(\frac{\partial^3 z}{\partial x^3}\Big)^2\Big]\Big\}\right\} -
\end{aligned}$$

$$
\begin{aligned}
&-2\beta_0\gamma\Big\{2\frac{\partial^3 z}{\partial x^3}\Big(\frac{\partial^4 y}{\partial x^3\partial t}\frac{\partial^2 z}{\partial x^2}+\frac{\partial^3 y}{\partial x^3}\frac{\partial^3 z}{\partial x^2\partial t}\Big)+\frac{\partial^3 y}{\partial x^3}\frac{\partial^3 z}{\partial x^2\partial t}+\\
&+2\frac{\partial^3 y}{\partial x^3}\frac{\partial^2 z}{\partial x^2}\frac{\partial^4 z}{\partial x^3\partial t}+\frac{\partial^3 y}{\partial x^2\partial t}\Big[3\Big(\frac{\partial^3 y}{\partial x^3}\Big)^2+\Big(\frac{\partial^3 z}{\partial x^3}\Big)^2+\frac{\partial^2 z}{\partial x^2}\frac{\partial^4 z}{\partial x^4}\Big]+\\
&+\frac{\partial^2 y}{\partial x^2}\Big(6\frac{\partial^3 y}{\partial x^3}\frac{\partial^4 y}{\partial x^3\partial t}+2\frac{\partial^3 z}{\partial x^3}\frac{\partial^4 z}{\partial x^3\partial t}+\frac{\partial^3 z}{\partial x^2\partial t}\frac{\partial^4 z}{\partial x^4}+\frac{\partial^2 z}{\partial x^2}\frac{\partial^5 z}{\partial x^4\partial t}\Big)\Big\}-\\
&-3\beta_0\Big\{\frac{\partial^3 y}{\partial x^2\partial t}\Big[3\Big(\frac{\partial^2 y}{\partial x^2}\Big)^2+\Big(\frac{\partial^2 z}{\partial x^2}\Big)^2+3\frac{\partial y}{\partial x}\frac{\partial^3 y}{\partial x^3}+\frac{\partial z}{\partial x}\frac{\partial^3 z}{\partial x^3}\Big]+\\
&+2\frac{\partial^3 y}{\partial x^3}\Big(\frac{\partial^2 z}{\partial x\partial t}\frac{\partial^2 z}{\partial x^2}+\frac{\partial z}{\partial x}\frac{\partial^3 z}{\partial x^2\partial t}\Big)+\\
&+2\frac{\partial^4 y}{\partial x^3\partial t}\frac{\partial z}{\partial x}\frac{\partial^2 z}{\partial x^2}+\frac{\partial^2 y}{\partial x^2}\Big(3\frac{\partial^2 y}{\partial x\partial t}\frac{\partial^3 y}{\partial x^3}+\frac{10}{3}\frac{\partial y}{\partial x}\frac{\partial^4 y}{\partial x^3\partial t}+\\
&+2\frac{\partial^2 z}{\partial x^2}\frac{\partial^3 z}{\partial x^2\partial t}+\frac{\partial^2 z}{\partial x\partial t}\frac{\partial^3 z}{\partial x^3}+\frac{\partial z}{\partial x}\frac{\partial^4 z}{\partial x^3\partial t}\Big)\Big\}-\\
&-2\gamma\Big\{2\frac{\partial^3 y}{\partial x^3}\frac{\partial^2 z}{\partial x^2}\frac{\partial^3 z}{\partial x^3}+\frac{\partial^2 y}{\partial x^2}\Big[3\Big(\frac{\partial^3 y}{\partial x^3}\Big)^2+\Big(\frac{\partial^3 z}{\partial x^3}\Big)^2+\frac{\partial^2 z}{\partial x^2}\frac{\partial^4 z}{\partial x^4}\Big]\Big\}\Big\}+\\
&+\Big[k_p\frac{\partial^2 y(x_s)}{\partial x^2}+k_d\frac{\partial^3 y(x_s)}{\partial x^2\partial t}\Big]\Big[\frac{\partial\delta(x-x_1)}{\partial x}-\frac{\partial\delta(x-x_2)}{\partial x}\Big]\Big[1-\frac{1}{2}\Big(\frac{\partial y}{\partial x}\Big)^2\Big]\cdot\\
&\cdot\Big[k_p\frac{\partial^2 y(x_s)}{\partial x^2}+k_d\frac{\partial^3 y(x_s)}{\partial x^2\partial t}\Big]\frac{\partial y}{\partial x}\frac{\partial^2 y}{\partial x^2}[\delta(x-x_1)-\delta(x-x_2)]=0
\end{aligned}
\tag{5.3}
$$

where η denotes the coefficient of external damping and $\delta(\cdot)$ is Dirac's delta function. The second equation of motion (for z) can be directly obtained from the above by replacing y with z and vice versa, and by exchanging the sign "$-$" for "$+$" and "$+$" for "$-$" before the terms multiplied by ω.

6. Stability analysis

In the following study the considerations will be focused on stability analysis of a PFC rotating shaft. A schematic representation of the shaft structure to be dealt with is shown in Fig. 8.

In order to examine the stability of the assumed system, the equations of motion, see (5.3), will be transformed into a set of ordinary differential equations by making use of a unimodal Galerkin's discretisation (orthogonalisation). The discretisation will be done with the first eigenform of a simply supported shaft taken as the base function. Let (5.3) be represented in the

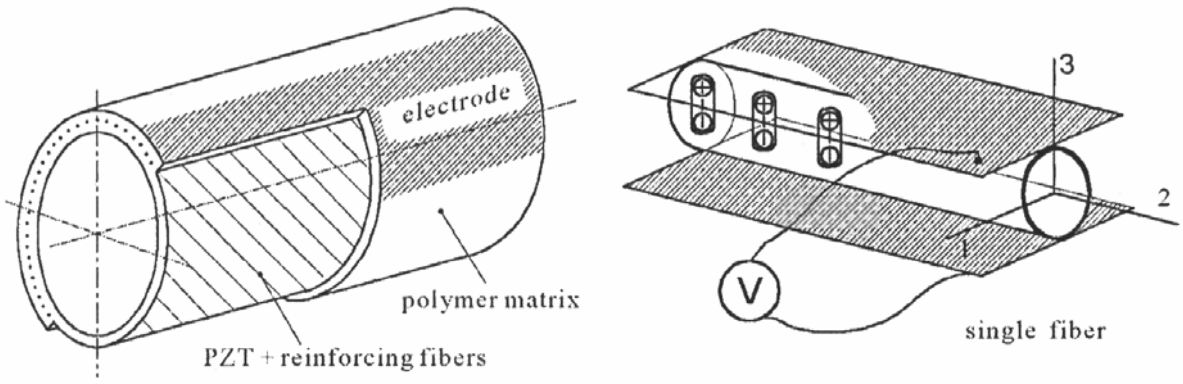

Fig. 8. Scheme of a PFC shaft with transversely poled piezoelectric fibers

form of differential operators $L_i[y(x,t), z(x,t)]$, $i = 1,2$. Let the solution to (5.3) be predicted as $y(x,t) = w_1(t)F(x)$ and $z(x,t) = w_2(t)F(x)$, where $F(x) = \sin(\pi x/l)$ and $w_1(t)$, $w_2(t)$ – arbitrary time functions. Galerkin's discretisation implies

$$\int_0^l L_i\Big\{y[F(x), w_1(t)], z[F(x), w_2(t)]\Big\}F(x)\,dx = 0 \qquad i = 1,2 \qquad (6.1)$$

which leads to a set of two second-order ordinary differential equations with respect to w_1 and w_2.

As the shaft undergoes a constant transverse load due to the force of gravity $q = \rho Ag$, its static equilibrium is a deflected plane curve representing the so-called non-trivial equilibrium position. It can be determined from discretised equations of motion by substituting $\dot{w}_1 = 0$, $\dot{w}_2 = 0$, $\ddot{w}_1 = 0$, $\ddot{w}_2 = 0$ and $w_1 = w_{10}$, $w_2 = w_{20}$. In fact w_{10} and w_{20} depend on the angular velocity of the shaft and create a kind of equilibrium curve against the function of ω.

The knowledge of the non-trivial equilibrium position is fundamental for further stability analysis. It is to be done in terms of eigenvalues corresponding to the matrix of the equations of motion linearised around the non-trivial equilibrium position. To make the analysis easier, introduce now new variables enabling transformation of the second-order ordinary differential equations of motion into four first-order ones, but linearised around the trivial position. It is possible when: $u_1 = w_1 - w_{10}$, $u_2 = \dot{w}_1$, $u_3 = w_2 - w_{20}$, $u_4 = \dot{w}_2$. The final but implicit form of the approximate equations of motion can be expressed as follows

$$\dot{\boldsymbol{u}} = \mathbf{A}(\omega; k_p, k_d)\boldsymbol{u} + \boldsymbol{N}(\boldsymbol{u}, \omega; k_p, k_d) = \boldsymbol{f}(\boldsymbol{u}, \omega; k_p, k_d) \qquad (6.2)$$

where $\mathbf{A}$ denotes the matrix of the linear part of the equations of motion, $\boldsymbol{N}$ – non-linear part, $\boldsymbol{f}$ full representation of their right-hand sides. Naturally:

$\boldsymbol{u} = [u_1, ..., u_4]^\top$, $\boldsymbol{N} = [N_1, ..., N_4]^\top$, $\boldsymbol{f} = [f_1, ..., f_4]^\top$ and $\mathbf{A} = \mathbf{A}_{4\times 4}$. In (6.2) the angular velocity as well as the gains k_p and k_d have been inserted into parentheses to emphasise that both linear and non-linear parts depend on these factors. To show this, find an explicit form of $\mathbf{A}$

$$\mathbf{A} = \begin{bmatrix} 0 & 1 & 0 & 0 \\ a_{21} & a_{22} & a_{23} & a_{24} \\ 0 & 0 & 0 & 1 \\ a_{41} & a_{42} & a_{43} & a_{44} \end{bmatrix} \tag{6.3}$$

where

$$\begin{aligned}
a_{21} &= -\pi^3(\pi + 2k_p \sin \pi x_s) + w_{10}^2 \pi^5 \Big[\frac{9}{4}(1 + \pi^2\gamma) + 3k_p \sin \pi x_s\Big] + \\
&+ \frac{3}{8} w_{20}^2 \pi^6 (1 + 2\pi^2\gamma) + \frac{3}{2} w_{10} w_{20} \pi^6 \omega \xi (1 + \pi^2\gamma) \\
a_{22} &= -\eta - \pi^4 \xi - 2\pi^3 k_d \sin \pi x_s + \\
&+ w_{10}^2 \pi^5 \Big[\frac{3}{4}\pi\xi(2 + 3\pi^2\gamma) + k_d \sin \pi x_s\Big] + \frac{3}{8} w_{20}^2 \pi^6 \xi (1 + 2\pi^2\gamma) \\
a_{23} &= -\pi^4 \xi\omega + \frac{3}{4} w_{10}^2 \pi^6 \xi\omega (1 + \pi^2\gamma) + \frac{9}{8} w_{20}^2 \pi^6 \xi\omega (1 + 2\pi^2\gamma) \\
a_{24} &= \frac{3}{4} w_{10} w_{20} \pi^6 \xi (1 + 2\pi^2\gamma) \\
a_{41} &= \pi^4 \xi\omega - \frac{9}{8} w_{20}^2 \pi^6 \xi\omega (1 + 2\pi^2\gamma) - \frac{3}{4} w_{10}^2 \pi^6 \xi\omega (1 + \pi^2\gamma) \\
a_{42} &= a_{24} \\
a_{43} &= -\pi^3(\pi + 2k_p \sin \pi x_s) + \frac{3}{8} w_{10}^2 \pi^6 (1 + 2\pi^2\gamma) + \\
&+ w_{20}^2 \pi^5 \Big[\frac{9}{4}(1 + \pi^2\gamma) + 3k_p \sin \pi x_s\Big] - \frac{3}{2} w_{10} w_{20} \pi^6 \omega \xi (1 + \pi^2\gamma) \\
a_{44} &= -\eta - \pi^4 \xi - 2\pi^3 k_d \sin \pi x_s + \frac{3}{8} w_{10}^2 \pi^6 \xi (1 + 2\pi^2\gamma) + \\
&+ w_{20}^2 \pi^5 \Big[\frac{3}{4}\pi\xi(2 + 3\pi^2\gamma) + k_d \sin \pi x_s\Big]
\end{aligned} \tag{6.4}$$

Application of Hurwitz's criterion to the linearised part of the governing equations leads to the characteristic equation of the fourth order. Its solution yields four complex eigenvalues (two conjugate pairs) which decide about stability of the system. Concentrate now on the eigenvalue having the greatest real part. It is the decisive eigenvalue, and will be denoted by r_1. The system is said to be stable if $\mathcal{R}e\{r_1\} < 0$.

A blow-up of the trajectories of the decisive eigenvalue is presented in Fig. 9 and Fig. 10. The eigenvalue moves rightwards for increasing rotation speed. It starts from the area where $\mathcal{R}e\{r_1\} < 0$, then intersects the imaginary axis, and finally gets positive real part (which entails loss of the stability and initiates flutter-type vibration). The ordinate, i.e. imaginary part, corresponds to the initial frequency of the self-excited vibration. As it can be seen, however, the application of control shifts the trajectories leftwards, i.e. stabilises the system (for moderate ω $\mathcal{R}e\{r_1\}$ becomes negative again). This effect is observed for both control strategies (proportional and differential). The differential approach (k_d) does not affect the initial flutter frequency and the proportional one (k_p) increases it (additional damping is introduced in the first case, additional stiffness in the second one).

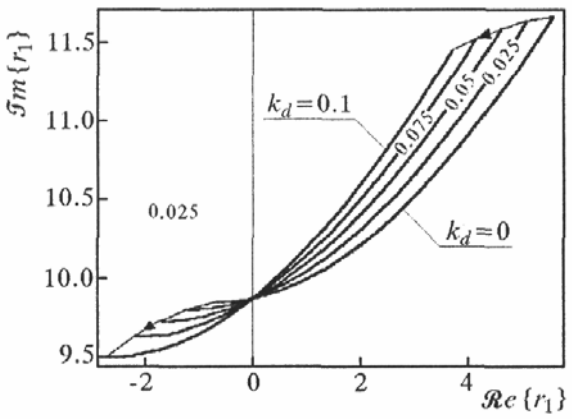

Fig. 9. Trajectories of the decisive eigenvalue for velocity feedback

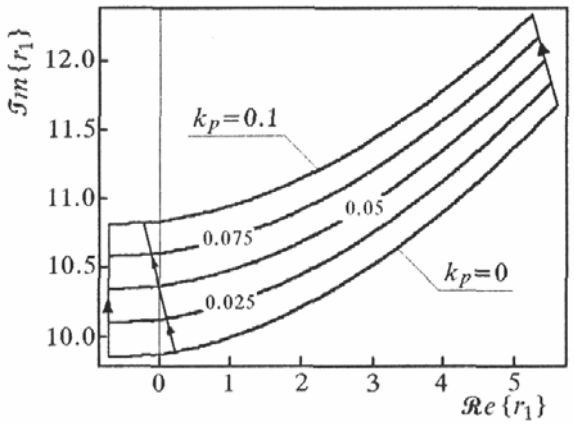

Fig. 10. Trajectories of the decisive eigenvalue for proportional feedback

The effect of both strategies on the increase of the critical rotation speed, at which self-excitation appears, is shown in Fig. 11 and Fig. 12. These diagrams disclose ω_{cr} as the function of the gains k_p and k_d as well as the lamination angle.

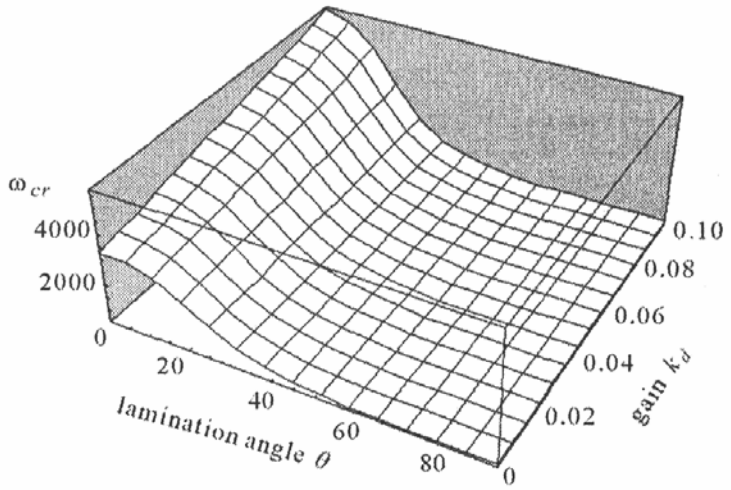

Fig. 11. Critical rotation speed for velocity feedback

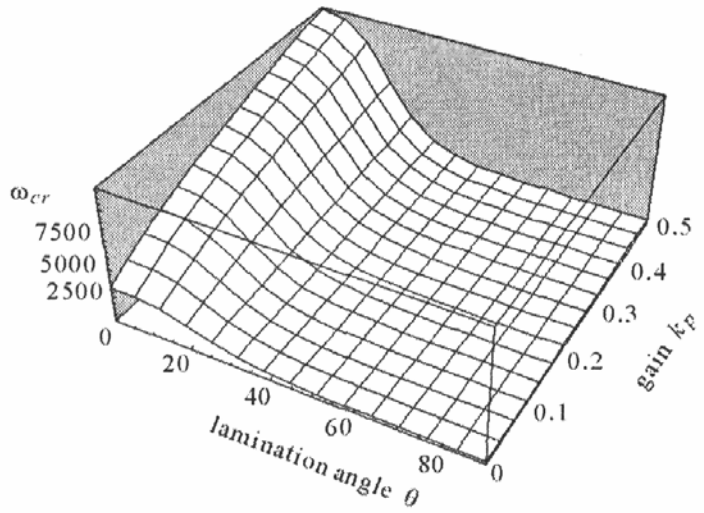

Fig. 12. Critical rotation speed for proportional feedback

This effect is even more visible on the plane stretched over the angular velocity and lamination angle, see Fig. 13 and Fig. 14.

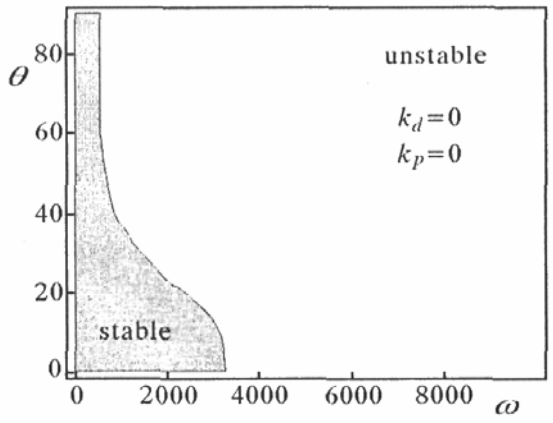

Fig. 13. Stability domain for disabled control system

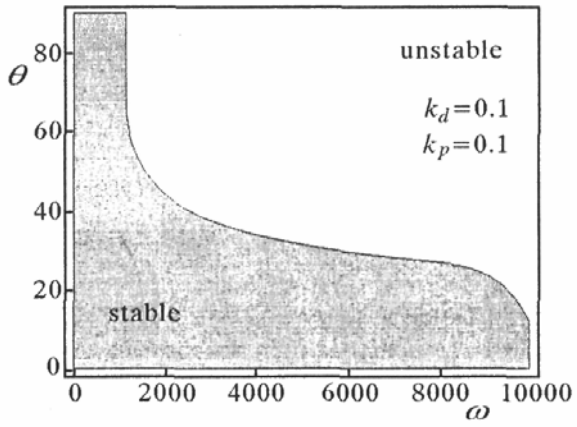

Fig. 14. Enlargement of the stability domain for enabled control system

7. Concluding remarks

In this paper the fundamentals of active flutter suppression, i.e. stabilisation and reduction of transverse vibration in a rotating shaft have been presented. A novel method has been incorporated. It consists in making use of active composite materials containing piezoelectric fibers able to produce mechanical stress and strain under an electric signal. Piezoelectric fiber composites are state-of-the-art modern "smart" materials which have freshly emerged in the field of mechatronics. They combine the advantages pertaining to laminates with new adaptive and controllable properties featured by piezoelectric elements.

Two degressive non-linearities have been taken into account: moderate curvature and ovalisation of the shaft cross-section during bending (Brazier's effect). The principle of generation of a bending moment in a rotating shaft

and governing equations have been discussed in detail. It occurred that the application of only three actuating electrodes around the shaft perimeter is enough to produce a constant counter-bending moment, despite the rotary motion of the entire structure. Such a moment opposes the internal interactions in the shaft that lead directly to self-excitation while exceeding the critical angular velocity. Closer analysis has confirmed that both proposed methods of stabilisation, i.e. these based on the proportional and velocity feedback, are effective in increasing the critical threshold. Irrespective of the electrode arrangement (transverse or interdigitated), it has occurred that smaller lamination angles are most efficient in reaching this goal, i.e. increasing ω_{cr} twice as much or even more.

References

1. ALDRAIHEM O.J., WETHERHOLD R.C., 1997, Mechanics and control of bending and twisting vibration of laminated beams, *Smart Materials and Structures*, **6**, 123-133

2. ASHTON J.E., HALPIN J.C., PETIT P.H., 1969, *Primer on Composite Materials: Analysis*, Technomic Publishing, Westport

3. BAUCHAU O.A., 1980, Optimal design of high-speed rotating graphite/epoxy shafts, *Journal of Composite Materials*, **17**, 170-181

4. BENT A.A., HAGOOD N.W., RODGERS J.P., 1995, Anisotropic actuation with piezoelectric fiber composites, *Journal of Intelligent Material Systems and Structures*, **6**, 3, 338-349

5. BIRMAN V., BERT C.W., 1987, Non-linear beam-type vibrations of long cylindrical shells, *International Journal on Non-Linear Mechanics*, **22**, 327-334

6. DAMJANOVIČ D., NEWNHAM R.E., 1992, Electrostrictive and piezoelectric materials for actuator applications, *Journal of Intelligent Material Structures and Systems*, **3**, 4, 190-208

7. HAHN H.T., 1980, Simplified formulas for elastic moduli of unidirectional continuous fiber composites, *Composite Technology Review*, **2**, 3, 5-7

8. IOOSS G., JOSEPH D.D., 1980, *Elementary Stability and Bifurcation Theory*, Springer-Verlag, New York

9. JIANG B., BATRA R.C., 2002, Effective properties of a piezocomposite containing shape memory alloy and inert inclusions, *Continuum Mechanics and Thermodynamics*, **14**, 1, 87-111

10. JIANG C.P., CHEUNG Y.K., 2000, An exact solution for the three-phase piezoelectric cylinder model under antiplane shear and its applications to piezoelectric composites, *International Journal of Solids and Structures*, **38**, 4777-4796

11. JONES R.M., 1975, *Mechanics of Composite Materials*, McGraw-Hill Scripta Book, Washington

12. KURNIK W., 1988, Bifurkacyjne drgania samowzbudne w układach mechanicznych, *Prace Naukowe Politechniki Warszawskiej, Mechanika*, **109**

13. KURNIK W., 1993, Self-excited vibration of thin-walled composite shafts with Brazier's effect, *Machine Dynamics Problems*, **6**, 125-140

14. KURNIK W., 1995a, Optimum design of a thin-walled laminated rotating shaft, *Machine Dynamics Problems*, **13**, 19-30

15. KURNIK W., 1995b, Simplified analysis of displacements, load capacity and damping of laminated shafts, *Machine Dynamics Problems*, **13**, 31-45

16. KURNIK W., PRZYBYŁOWICZ P.M., 2001, Stability of rotating columns made of active fiber composites subject to follower loads, *Zbiór referatów konferencji "Polska Mechanika u Progu XXI Wieku"*, ed. W. Szcześniak, Kazimierz Dolny, 311-316

17. KURNIK W., PRZYBYŁOWICZ P.M., 2002, Active stabilisation of a piezoelectric fiber composite shaft subjected to follower load, *Proceedings of Seventh Pan-American Congress of Applied Mechanics PACAM VII*, Eds. P. Kittl, G. Diaz, D. Mook, J. Geer, Temuco, Chile, 93-96

18. KURNIK W., TYLIKOWSKI A., 1997, *Mechanika elementów laminowanych*, Oficyna Wydawnicza Politechniki Warszawskiej

19. MUSZYŃSKA A., 1971, Z zagadnień dynamiki wirników, *Prace Instytutu Podstawowych Problemów Techniki PAN*, **14**, 84-104

20. MUSZYŃSKA A., 1976, Motion of a shaft with nonlinear elastic and damping properties, *Zagadnienia Drgań Nieliniowych*, **17**, 189-224

21. NEWNHAM R.E., BOWEN K.A., KLICKER K.A., CROSS L.E., 1980, Composite piezoelectric transducers, *Material Engineering*, **2**, 93-106

22. NYE J.F., 1985, *Physical Properties of Crystals*, Oxford, Clarendon

23. PRZYBYŁOWICZ P.M., 1996, Aktywna stabilizacja flateru przewodów z przepływającym płynem za pomocą elementów piezoelektrycznych, *Zeszyty Naukowe Politechniki Rzeszowskiej, Mechanika*, **48**, II, 277-284

24. PRZYBYŁOWICZ P.M., 1998, Stability of a fast-moving wheelset – the role of internal friction, *Machine Dynamics Problems*, **20**, 221-229

25. PRZYBYŁOWICZ P.M., 1999a, Near-critical bifurcating vibration of a rotating shaft with piezoelectric elements, *Int. Journal Mechanics and Mechanical Engineering*, **3**, 2, 103-112

26. PRZYBYŁOWICZ P.M., 1999b, Aktywna stabilizacja wirującego wału za pomocą elementów piezoelektrycznych, *Zeszyty Naukowe Politechniki Rzeszowskiej, Mechanika*, **174**, 52, 207-214

27. PRZYBYŁOWICZ P.M., 2000, Effect of active stabilisation by piezoelectric elements on bifurcation of rotating shafts, *4th EUROMECH Solid Mechanics Conference*, Metz, France, *Book of Abstracts II*, M. Potier-Ferry, L.S. Toth, eds., General sessions, 576

28. PRZYBYŁOWICZ P.M., 2001a, Stabilizacja wirującego wału wykonanego z aktywnych elementów kompozytowych, *Zbiór referatów V Szkoły "Metody Aktywne Redukcji Drgań i Hałasu"*, Kraków-Krynica, 241-248

29. PRZYBYŁOWICZ P.M., 2001b, Stability of composite rotating shafts containing active piezoelectric fibers, *Book of Abstracts, IV German-Greek-Polish Symposium "Advances in Mechanics"*, Pułtusk, 52-53

30. PRZYBYŁOWICZ P.M., 2002, On stability of a thin-walled shaft with active piezoelectric fibers, *PAMM – Proceedings in Applied Mathematics and Mechanics*, Wiley InterScience, **1**, 1, 89-90

31. REISSNER E., 1959, On Finite bending of pressurized tubes, *Journal of Applied Mechanics*, **26**, 386-392

32. SPORN D., SCHOENCKER A., 1999, Composites with piezoelectric thin fibers – first evidence of piezoelectric behaviour, *Materials Research Innovations*, **2**, 303-308

33. TONDL A., 1965, *Some Problems of Rotor Dynamics*, Chapman and Hall, London

34. TYLIKOWSKI A., 1980, Dynamic stability of a rotating shaft, *Ingenieur Archiv*, **49**, 214-221

35. TYLIKOWSKI A., 1993, Dynamic stability of rotating angle-ply composite shafts, *Machine Dynamics Problems*, **6**, 141-156

36. WANG L., ZHU J., ZOU X., ZHANG F., 2000, PbTiO3-P(VDF-TeFE) composites for piezoelectric sensors, *Sensors and Actuators B(Chemical)*, **66**, 266-268

37. XIANG-DONG CHEN, DA-BEN YANG, YA-DONG JIANG, ZHI-MING WU, DAN LI, FU-JUN GOU, JIA-DE YANG, 1998, 0-3 piezoelectric composite film with high d_{33} coefficient, *Sensors and Actuators A(Physical)*, **65**, 194-196

38. YU N., 1999, On overall properties of smart piezoelectric composites, *Composites: Part B (Engineering)*, **30**, 709-712

Stateczność wirujących wałów wykonanych z aktywnego laminatu zawierającego włókna piezoelektryczne

Streszczenie

W pracy przedstawiono teoretyczne podstawy stabilizacji wirującego wału za pomocą elementów piezoelektrycznych. Wał jest wykonany z aktywnego laminatu zawierającego włókna piezoelektryczne – najnowszego osiągnięcia inżynierii materiałowej na polu mechatroniki. Niezależnie od rodzaju materiału, z którego wykonano wał, wykazuje on niestateczność typu flatter wywołaną obecnością tarcia wewnętrznego. Przy pewnej krytycznej prędkości wirowania układ traci stateczność, stając się narażonym na drgania samowzbudne. W artykule przeprowadzono dyskusję nad możliwością ochrony wirujących wałów przed takim zjawiskiem lub przynajmniej odsunięciem progu krytycznego poprzez zastosowanie włókien piezoelektrycznych zatopionych w materiale osnowy kompozytu wyposażonego w elektrody sterujące polem elektrycznym w każdej warstwie laminatu. Analiza zaprezentowanej metody stabilizacji pokazała, że wprowadzenie trzech i więcej par elektrod wystarcza do generowania stałego momentu gnącego mimo ciągłego wirowania. W układzie sterowania zastosowano pętlę ze sprzężeniem proporcjonalnym i prędkościowym. Wartość krytycznej prędkości wirowania znaleziono poprzez śledzenie trajektorii wartości własnych równań dynamiki zlinearyzowanych wokół nietrywialnego położenia równowagi. Równania te wyprowadzono wychodząc z cząstkowych różniczkowych równań ruchu wału po ich jedno-modalnej dyskretyzacji Galerkina. Pokazano, że zastosowana metoda stabilizacji jest efektywna i pozwala na ponad dwukrotne zwiększenie progu krytycznego.

Manuscript received May 24, 2002; accepted for print July 3, 2002